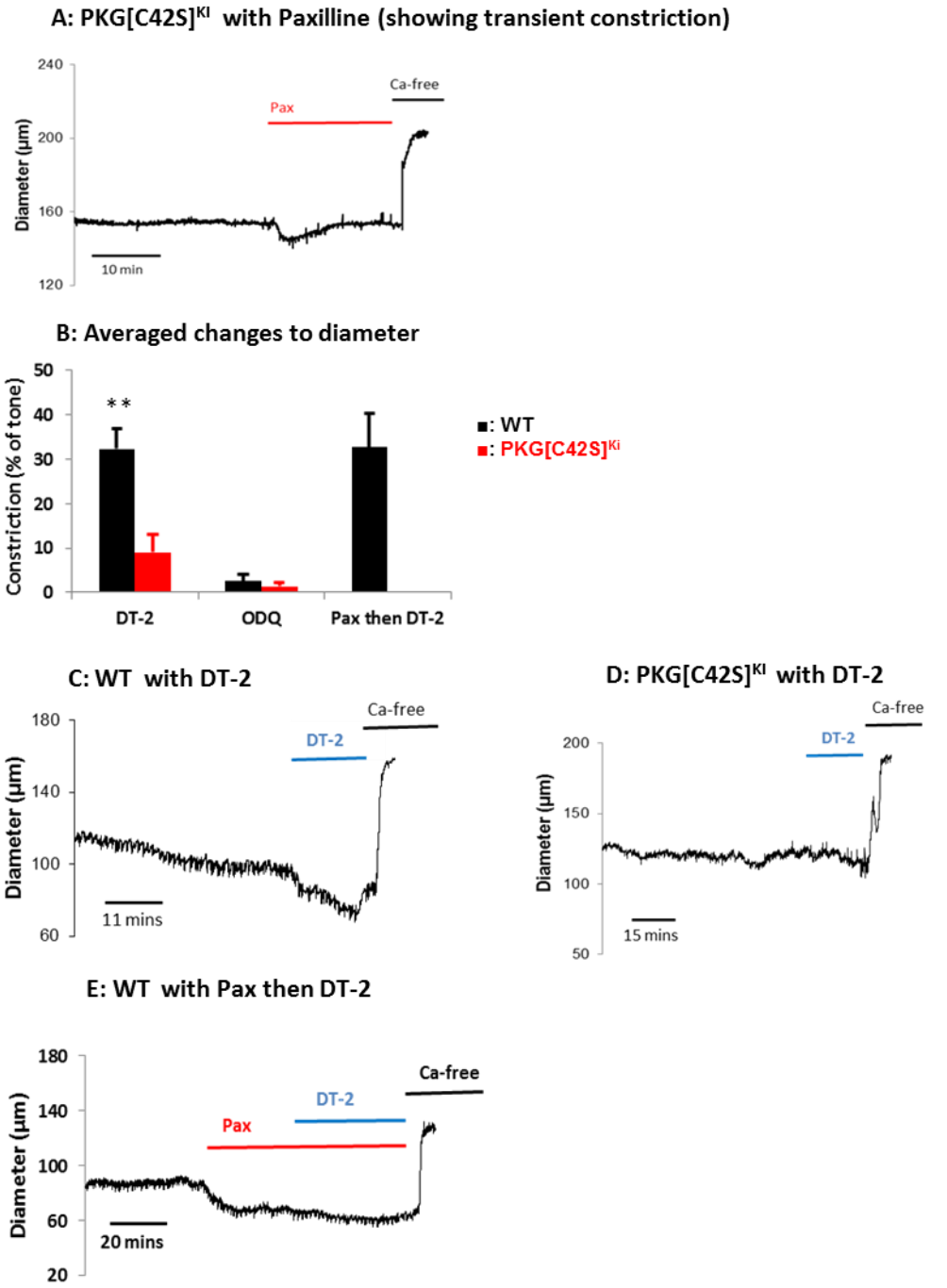

Supplementary Figure 1: Oxidant-activated PKG is required for BK channel activity to oppose pressurize-induced constriction.

A. Representative example of a small, transient constriction occasionally seen in pressure-constricted mesenteric arteries from PKG[C42S]^{KI} mice. B: Constriction of WT and PKG[C42S]^{KI} arteries to the direct PKG inhibitor DT-2 (WT, n = 6 arteries from 6 mice; PKG[C42S]^{KI}, n = 4 arteries from 4 mice; $P = 0.007$), the sGC inhibitor ODQ (WT, n = 3 arteries from 3 mice; PKG[C42S]^{KI}, n = 3 arteries from 3 mice; not significant) and paxilline followed by DT-2 (n = 4 arteries from 4 WT mice). C. Representative diameter recordings of a pressure-constricted mesenteric artery from a WT mouse incubated with DT-2 (3 µM). D: Representative diameter recordings of a PKG[C42S]^{KI} pressure-constricted mesenteric artery incubated with DT-2 (3 µM). E. Representative diameter recordings of a WT mesenteric artery constricted first with paxilline (1 µM) and then co-incubated with DT-2 (3 µM).

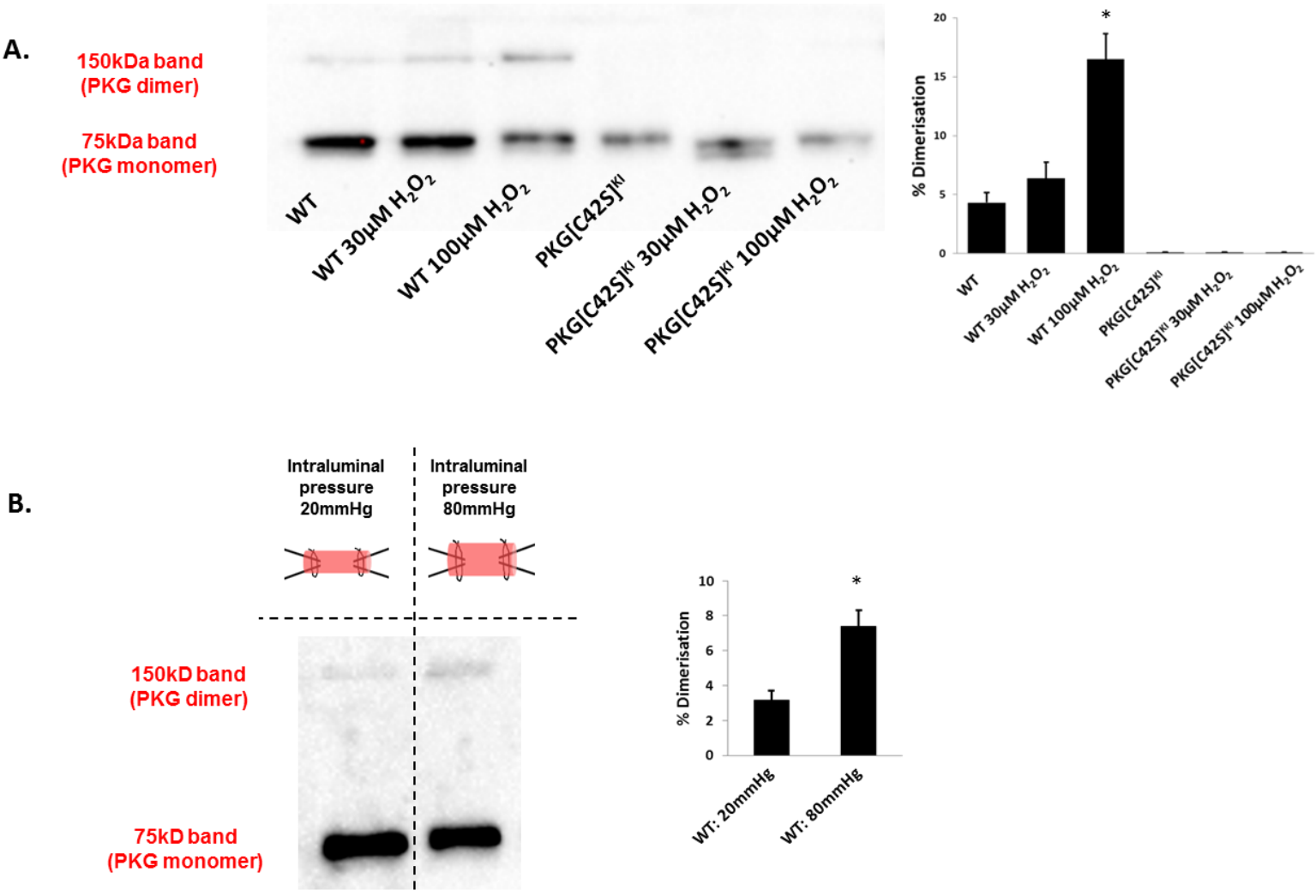

Supplementary Figure 2: Oxidative dimerization of PKG in arteries exposed to pressure and H_2O_2.

A: Representative western blot (left) and summary data showing overall amounts (right) of dimerized PKG from freshly dissected, pooled (unpressurized) mesenteric arteries in response to incubation with H_2O_2, presented as means ± SEM (*P < 0.01, compared with no-H_2O_2 control; WT, n = 9 arteries from 9 mice; WT + 30 µM H_2O_2, n = 5 arteries from 5 mice; WT + 100 µM H_2O_2, n = 9 arteries from 9 mice). B. Representative western blot (left) and summary data showing overall amounts (right) of dimerized PKG from individual WT arteries pressurized to 20 (n = 8 arteries from 8 mice) or 80 mmHg (n = 8 arteries from 8 mice) (*P = 0.04 compared with 20 mmHg).

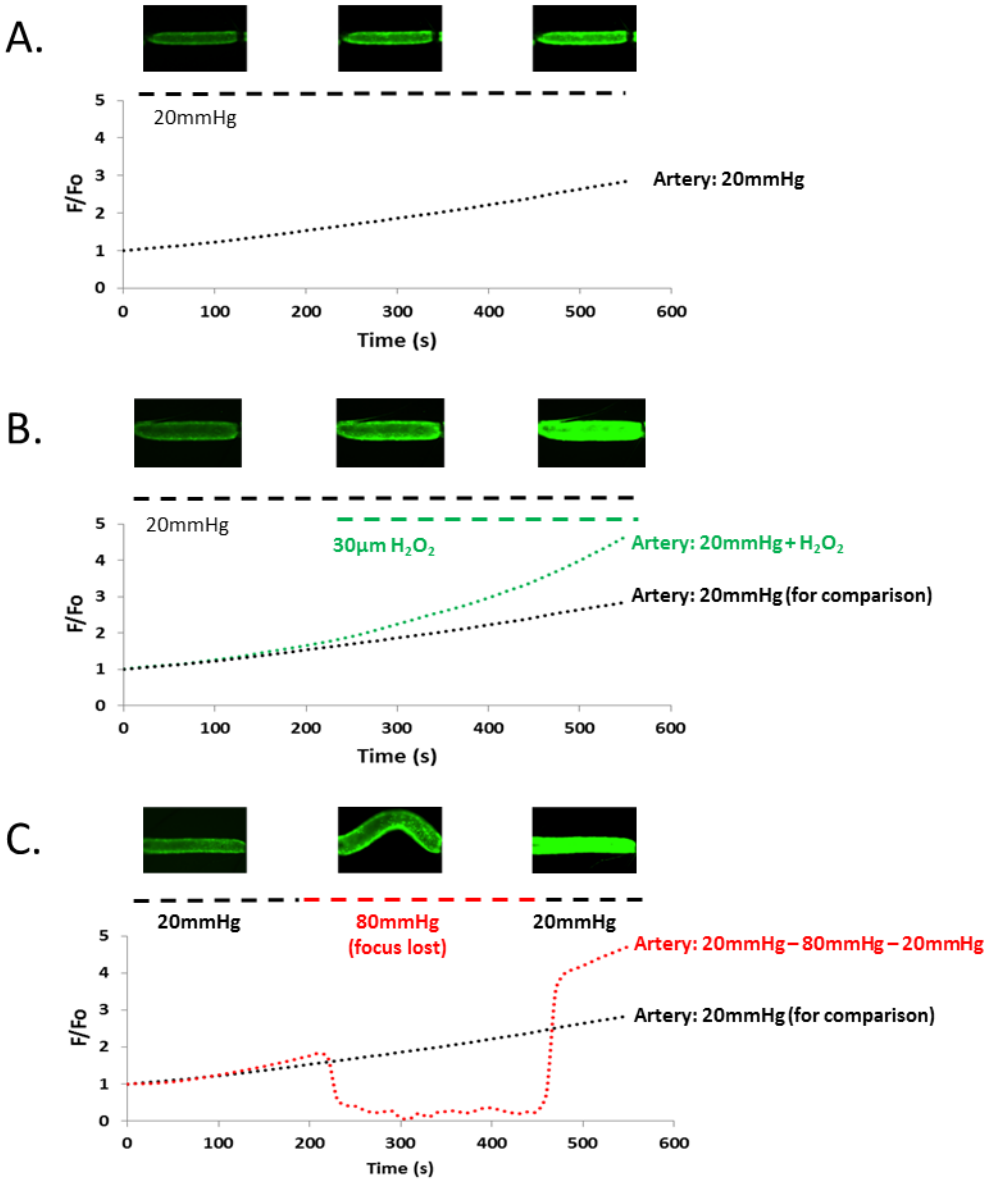

Supplementary Figure 3: Intraluminal pressure increases oxidant amounts in mesenteric arteries.

A: Representative trace showing the rate in the increase in fluorescence in CM-H_2DCFDA – loaded WT arteries pressurized at 20 mmHg. B: Representative trace showing the increase in fluorescence in CM-H_2DCFDA WT arteries pressurized at 20 mmHg with exogenous application of the oxidant 30 µM H_2O_2 (at 240 seconds); end point comparisons at 9 minutes: 20 mmHg control (F/F_o = 3.0 ± 0.3) compared to 20 mmHg + H_2O_2 (F/F_o = 4.2 ± 0.3; n = 4 arteries from 4 mice, *P* = 0.01). C: Representative trace showing the increase in fluorescence in CM-H_2DCFDA WT arteries pressurized initially at 20 mmHg, then subject to 80 mmHg (210 –480 seconds) and finally returned to 20 mmHg (to control for surface area and tissue density/longitudinal stretch); end point comparisons at 9 minutes: 20 mmHg (F/F_o = 3.0 ± 0.3) compared to 80 mmHg (F/F_o = 4.3 ± 0.2; n = 4 arteries from 4 mice, p = 0.01).

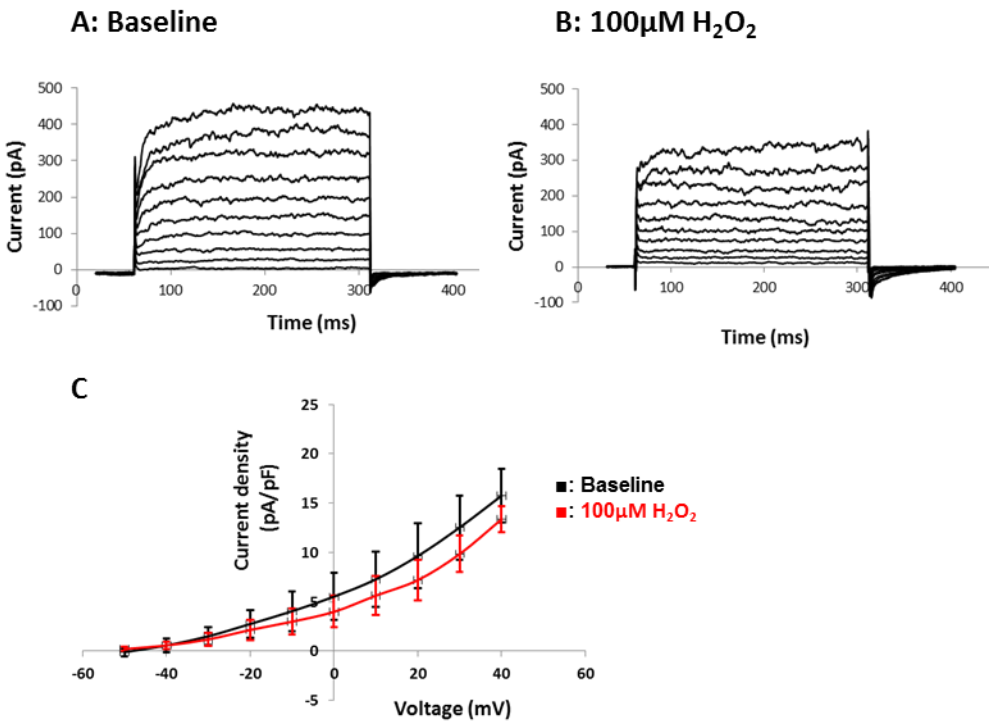

Supplementary Figure 4: H_2O_2 has no effect on K^+ currents in the absence of Ca^{2+} sparks.
A: Representative trace of outward currents from WT mesenteric VSMCs elicited by a voltage step protocol (10-mV, 250-ms steps from a holding potential of -80 mV), measured in the perforated-patch configuration in the presence of ryanodine and nifedipine (20 µM each). B: Representative trace of outward currents elicited from WT mesenteric VSMCs by a voltage step protocol after incubation with 100 µM H_2O_2 (a concentration that causes oxidative disulphide bond formation between the cysteine residues within the PKG dimer), measured in the whole-cell configuration in the presence of 20 µM ryanodine. C: Current density–voltage relationship for VSMCs before and after incubation with H_2O_2 (n=3 cells from 3 mice). There was no significant difference in outward currents between baseline and H_2O_2 treatment.

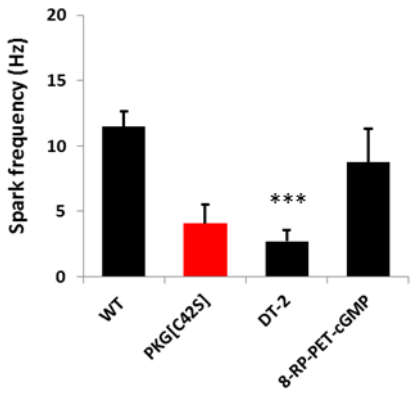

Supplementary Figure 5: Pharmacological manipulation of Ca^{2+} sparks.

DT-2 (3 μm) significantly reduced Ca^{2+} spark frequency in intact arteries pressurized at 80 mmHg (*$p < 0.01$, compared to WT), but this effect was not observed with the cGMP antagonist 8-RP-PET-cGMP (WT, n = 8 arteries from 7 mice; PKG[C42S], n = 14 arteries from 11 mice; DT-2, n = 9 arteries from 9 mice; 8-RP-PET-cGMP, n = 7 arteries from 7 mice).

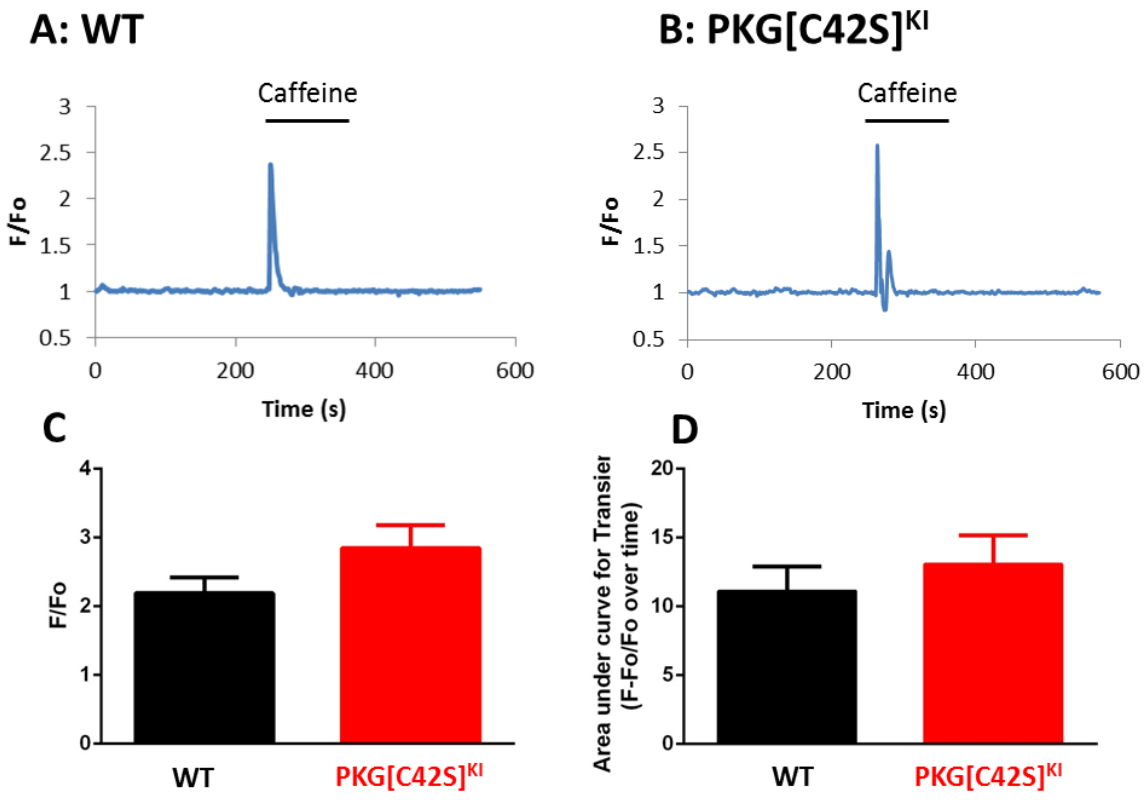

Supplementary Figure 6: Caffeine induced Ca^{2+} transients in WT and PKG[C42S]^{KI} mesenteric arteries

A and B: Representative traces of changes to fractional fluorescence (F/Fo) following application of 10 mM caffeine. C: Comparison of caffeine peak amplitude (F/Fo) between WT (n=4 arteries from 3 mice) and PKG[C42S]KI (n=5 arteries from 3 mice). D: Comparison of the Area under the curve (AUC) for each caffeine peak between WT (n=4 arteries from 3 mice) and PKG[C42S]KI (n=5 arteries from 3 mice)

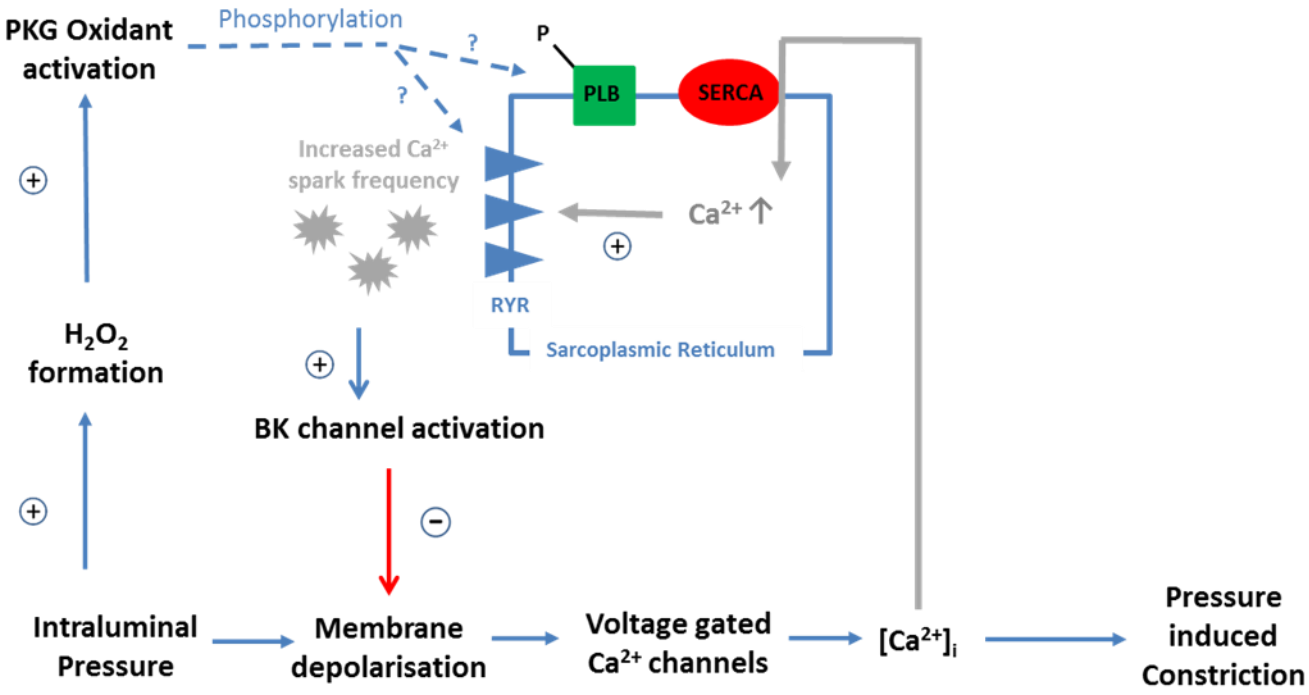

Supplementary Figure 7: Working model for the role of PKG and pressure-induced ROS.
Intraluminal pressure results in formation of H_2O_2, which causes oxidative disulfide bond formation between appositioned cysteine residues within a PKG dimer and thus activates the kinase. Once activated, PKG works in conjunction with membrane depolarization to sustain physiological amounts of Ca^{2+} spark activity. Blue triangles within the sarcoplasmic reticulum represent ryanodine receptors.